FRIGID ZONE **MEDICINE**
Original Article • DOI: 10.1515/fzm-2025-0004

Metabolomics study on dibenz[a,h]anthracene exposure-induced pulmonary injury in rats after intratracheal instillation

Zhen Kang[1,2], Qianqi Hong[1,2], Fei Yan[2], Tianyi Yu[2], Yuna Bai[2], Xiaobo Liu[2], Xiaolin Na[1*], Cheng Wang[1*]

Abstract

Background: Northern residents predominantly rely on coal-fired heating during winter, leading to severe air pollution. Polycyclic aromatic hydrocarbons (PAHs) adsorbed on atmospheric particulate matter pose significant health risks. Among PAHs, dibenz[a,h]anthracene (DahA), though present at lower environmental concentrations compared to other PAHs, exhibits a carcinogenic potency that is 10 or more times greater than benzo[a]pyrene (BaP), underscoring its potential harm. Despite reports on DahA's multiple toxic effects, its impact on metabolic networks remains poorly understood. **Methods:** Based on the respiratory volume of adult rats and the concentration of $PM_{2.5}$-bound DahA in heavily polluted cities of northern China, adult Sprague-Dawley rats were treated with DahA (0.07 μg/kg and 0.2 μg/kg) twice weekly for four weeks *via* intratracheal instillation. Metabolomic profiling of serum was performed using rapid resolution liquid chromatography coupled with quadrupole time-of-flight tandem mass spectrometry (RRLC/Q-TOF-MS) to elucidate metabolic disruptions caused by DahA exposure. **Results:** DahA exposure induced significant oxidative stress and inflammatory responses in rats, accompanied by notable alterations in the serum metabolome. A total of 11 metabolites were found to be decreased, and 2 metabolites were increased, with disruptions observed in folate biosynthesis, glycerophospholipid metabolism, and nitrogen metabolism pathways. Additionally, metabolic dysregulation may interfere with the tricarboxylic acid cycle and compromise nucleotide homeostasis. **Conclusion:** These findings enhance our understanding of the toxicological effects of DahA exposure and its role in lung damage. The results suggest that metabolic disturbances caused by DahA may contribute to the exacerbation of respiratory diseases associated with particulate matter-bound PAH pollution during the heating season in cold regions.

Keywords

DahA; metabolomics; pulmonary injury; heating season

Received 05 March 2024, accepted 05 August 2024

[1]*Department of Environmental Hygiene, School of Public Health, Harbin Medical University, Harbin 150081, China*
[2]*Department of Environmental Hygiene, Harbin Center for Disease Control and Prevention, Harbin 150026, China*

**Corresponding authors Cheng Wang, E-mail: wangchenghlj@163.com; Xiaolin Na, E-mail: naxiaolin1965@163.com*

1 Introduction

Northern China experiences a longer winter and lower average temperatures. Residents primarily rely on coal-fired heating, which contributes to frequent regional haze. Ambient $PM_{2.5}$-bound polycyclic aromatic hydrocarbons (PAHs), known for their high content and toxicity, have garnered significant attention. PAHs, predominantly generated from the combustion of organic materials and gasoline exhaust, are widely distributed atmospheric pollutants[1]. During the heating season, PAHs adsorbed onto atmospheric particulate matter have been associated with increased morbidity related to respiratory and cardiovascular diseases, as well as impairments in cognitive development and immune function[2-4].

In previous studies, PAHs have been identified as classic persistent organic environmental pollutants with mutagenic and carcinogenic properties, which can increase the risk of lung cancer, skin cancer, breast cancer, and oral cancer in the population[5-6]. Additionally, PAHs such as benz[a]anthracene (BaA), benzo[a]pyrene (BaP), benzo[b]fluoranthene (BbFA), and benzo[k]fluoranthene (BkFA) have been shown to exhibit

embryotoxicity in both *in vivo* and *in vitro* experiments. Maternal exposure to BbFA disrupted the expression of steroidogenesis-related genes, and testicular apoptosis mediators were significantly upregulated in young adult F1 mice[7]. Furthermore, BaA and BkFA were found to reduce the expression of estrogen receptor α in luminal epithelium, glandular epithelium, and stromal cells[8].

PAHs are mixtures; however, the responses elicited by each chemical component are distinct. Currently, most research on environmental PAHs has focused on BaP, with comparatively less attention given to fully characterizing the effects of dibenz[a,h] anthracene (DahA). DahA is also a component of PAH complexes and has been designated as a probable human carcinogen by IRIS[9]. A previous study found that ambient $PM_{2.5}$-bound DahA levels were correlated with small airway dysfunction in primary schoolchildren in northeast China[10]. Meanwhile, another study demonstrated that sub-chronic oral treatment with DahA resulted in the formation of fewer DNA adducts than BaP at the same dose, but with similar mutation induction[11]. Although the exposure concentrations of DahA in the air are much lower than those of other PAHs, animal studies indicate that the carcinogenic potency of DahA is 10 times (or more) greater than that of BaP[12]. Therefore, the potential harm of DahA should not be overlooked.

Currently, the metabolic mechanisms underlying DahA toxicity remain unclear. Previous studies have explored the metabolic impacts of water-soluble or insoluble components of $PM_{2.5}$ exposure in rats, identifying disrupted metabolic pathways, including lipid metabolism, amino acid metabolism, energy metabolism, stress hormone metabolites, and altered circadian rhythm biomarkers[13-15]. Despite these efforts, the metabolic mechanisms of individual PAHs, such as DahA, are still largely unknown, and limited research has been conducted on rat intratracheal instillation models for DahA toxicity exposure.

It is hypothesized that the level of Reactive Oxygen Species (ROS) may be increased by exogenous compounds, and in turn, pro-inflammatory cytokines and chemokines may be stimulated by the production of ROS and Reactive Nitrogen Species (RNS), leading to tissue damage[16-17]. Metabolites, as the terminal products of gene expression, play a critical role in cellular communication processes[18]. While metabolomics has been widely applied in lung-related clinical studies, its application in understanding PAH-induced lung toxicity remains limited. Therefore, the purpose of this study was to investigate oxidative stress and inflammation responses caused by the intratracheal instillation of DahA. A metabolomics approach based on rapid resolution liquid chromatography coupled with quadrupole time-of-flight tandem mass spectrometry (RRLC/Q-TOF/MS) was used to explore disruptions in serum metabolic profiles in rats. In conclusion, these findings enhance our understanding of the toxic effects of DahA exposure in the development of lung damage and provide insights into the mechanisms of environmental toxicity caused by PAHs.

2 Methods and materials

2.1 Chemicals

The chemical products used in this study included DahA (CAS 50-70-3), purchased from Tokyo Chemical Industry Co., Ltd. (Tokyo, Japan), with a purity of >98%. Assay kits for alkaline phosphatase (AKP), lactate dehydrogenase (LDH), total protein (TP), superoxide dismutase (SOD), malondialdehyde (MDA), nitric oxide synthase (iNOS, eNOS), and nitric oxide (NO) were obtained from Nanjing Jiancheng Bio-technology and Science Inc. (Nanjing, China). Kits for interleukin (IL-6) and tumor necrosis factor (TNF)-α were purchased from Boster Biological Technology Ltd. (Wuhan, China), and all reagents were used according to the manufacturer's protocols.

2.2 Animal care

Prior to the study initiation, the experimental protocol was reviewed and approved by the Committee on Animal Research and Ethics of Harbin Medical University (2015010). Twenty-four male Sprague-Dawley rats (6 weeks old, weighing 180-200 g) were purchased from Beijing WTLH Laboratory Animal Co., Ltd. (Beijing, China). After 1 week of acclimatization, the rats were randomly assigned to three groups (N = 8/group): the low-dose DahA-exposed (DL) group, high-dose DahA-exposed (DH) group, and the control group. The rats were exposed to DahA by intratracheal instillation twice a week for 4 weeks. The respiratory volume of adult rats was 0.105 m^3/day[16]. For heavily polluted northern Chinese cities, the reported levels of $PM_{2.5}$-bound DahA were approximately 6.49 ng/m^3. Taking into account the interspecies uncertainty factor (10-fold), the low-dose concentration of 0.07 μg/kg·bw was chosen, with a high-dose concentration set at 3 times this amount (0.2 μg/kg·bw).

2.3 Sample collection and preparation

After the final exposure, the rats were anesthetized with chloral hydrate. Blood was collected *via* the abdominal aorta, and serum samples were obtained by centrifugation (3500 g, 10 min at 4°C). The left bronchus was temporarily closed with a hemostatic clamp, and the right lung was lavaged with 3 mL of bronchoalveolar lavage fluid (BALF) three times. An aliquot of the recovered lavage fluid was then centrifuged (1500 rpm for 10 min at 4°C). Subsequently, a portion of the left lung was excised, fixed in 4% paraformaldehyde in PBS, and paraffin-embedded for Hematoxylin and Eosin (HE) staining analysis.

Before RRLC/Q-TOF/MS analysis, 1000 μL of acetonitrile was added to 200 μL of serum. After vortexing vigorously for 2 minutes, the mixture was allowed to settle at 20°C for 15 minutes and then centrifuged at 14,000 g for 15 minutes at 4°C. The supernatant was dried under nitrogen at 37°C. The residue was then dissolved in 300 μL of acetonitrile-water (3:1, v/v), vortex-mixed for 60 seconds, kept at 20°C for 10 minutes, and centrifuged again at 14,000 g for 15 minutes at 4°C. The supernatant was then transferred into a sample *vial* for RRLC/Q-TOF/MS analysis.

2.4 Chromatography and mass spectrometry

Chromatography and mass spectrometry analysis, biomarker identification, and potential target metabolic pathway analysis using MetaboAnalyst 3.0 were performed as previously described[19]. The raw RRLC-QTOF/MS ESI+ data were transformed into mzData files using MassHunter Qualitative Analysis Software (Agilent Technologies, USA), and these files were then imported into the XCMS package in R for preprocessing.

2.5 Data analysis

Statistical analysis was performed using SPSS (version 17.0; Beijing Stats Data Mining Co., Ltd., Beijing, China). Data are presented as mean ± Standard Deviation (SD). Differences between groups were analyzed using one-way analysis of variance (ANOVA). All *P*-values were two-tailed, and a P value < 0.05 was considered significant. The normalized data were exported to SIMCA-P (version 14.0; Umetrics AB, Umeå, Sweden) for multivariate data analysis.

3. Results

3.1 Physiological conditions

Body weights showed a normal increasing trend over the 4-week exposure period. Therefore, the body weight of the exposed groups was not significantly different from that of the control group at any time point (P > 0.05) (Table 1).

3.2 Pathology changes in lung tissue

Morphological alterations in the lungs were observed through HE staining, as shown in Fig. 1. Lung structures were nearly normal, with only slight lung inflammation in the control group (Fig. 1A). In contrast, pathological changes were more pronounced in the

Table 1 The fundamental variables between the control group and the DahA exposure group during the experiment

	Control (N = 8)	DL (N = 8)	DH (N = 8)
Body weight (g)	304.5 ± 15.7	298.4 ± 18.8	296.0 ± 23.4
Cytotoxicity and inflammation cytokine in BALF			
LDH (U/L)	121.51 ± 25.92	165.55 ± 70.02*	180.06 ± 61.27*
AKP (U/100mL)	3.48 ± 1.27	4.16 ± 1.18	7.08 ± 2.10*
TP (mg/L)	158.27 ± 59.60	190.47 ± 85.81*	242.05 ± 57.68*
IL-6 (pg/mL)	101.06 ± 28.57	126.15 ± 73.21	154.10 ± 42.51*
TNF-α (pg/mL)	28.15 ± 8.47	45.12 ± 10.59*	40.71 ± 18.81
Inflammatory and oxidant stress cytokine levels in serum			
SOD (mg/mL)	32.59 ± 3.65	21.74 ± 4.67*	17.55 ± 3.94*
MDA (mg/mL)	1.03 ± 0.30	1.17 ± 0.38	1.27 ± 0.38
IL-6 (pg/mL)	32.68 ± 14.52	47.27 ± 15.37	53.88 ± 18.66*
TNF-α (pg/mL)	22.14 ± 9.28	26.07 ± 11.34	27.46 ± 8.85
Markers of oxidative stress in rat lung tissue			
SOD (U/mg prot)	82.72 ± 18.84	60.53 ± 17.49*	55.47 ± 19.95*
MDA (nmol/mg prot)	1.51 ± 0.52	2.47 ± 0.55*	2.03 ± 0.46
i-NOS (U/mg prot)	0.58 ± 0.31	0.83 ± 0.32	1.21 ± 0.76*
e-NOS (U/mg prot)	2.13 ± 1.06	1.58 ± 0.85	1.37 ± 0.45
NO (nmol/mg prot)	1.71 ± 0.41	2.37 ± 0.53	2.91 ± 0.67*

DL: low-dose DahA-exposed; DH: high-dose DahA-exposed; BALF: bronchoalveolar lavage fluid; LDH: lactate dehydrogenase; AKP: alkaline phosphatase; TP: total protein; IL: Interleukin; TNF: tumor necrosis factor; SOD: Superoxide dismutase; MDA: malondialdehyde; NOS: nitric oxide synthase; NO: nitric oxide. *P value < 0.05 was considered significantly compared with the control group.

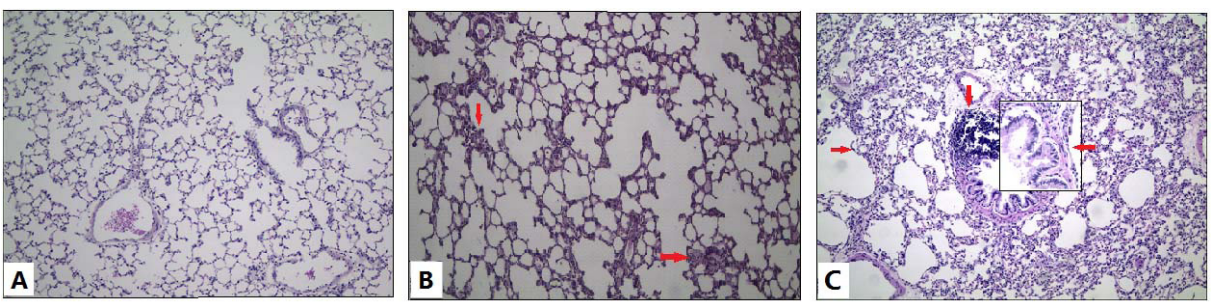

Fig. 1 Photomicrographs of rat lungs (HE staining)

(A) Control group: Lung structures appeared nearly normal with only slight inflammation; (B) DL group: Lung structures remained nearly normal, but inflammatory cell infiltration was more pronounced compared to the control group, as indicated by the arrows; (C) DH group: Compared with the control group, thickened alveolar walls and proliferation of fibrous tissue were observed, as indicated by the arrows in the exposed groups. Original magnification: ×200; small window in exposed group: ×400.

exposure groups. Inflammatory cell infiltration (Fig. 1B, C), thickened alveolar walls, and proliferation of fibrous tissue (Fig. 1C) were observed and are indicated by the arrows in the exposed groups.

3.3 Cytotoxic and proinflammatory cytokines in BALF

The mean values of cytotoxicity and inflammatory cytokines in BALF are shown in Table 1. To examine lung injury, cytotoxicity markers (LDH, AKP, TP) and proinflammatory factors (IL-6, TNF-α) in BALF were measured. The results showed that the levels of cytotoxicity markers (LDH, TP) in BALF were significantly increased in the exposure groups, and the level of AKP in the DH group was significantly higher compared to the control group ($P < 0.05$). Furthermore, the level of IL-6 in BALF was significantly upregulated in the DH group, and the level of TNF-α in BALF was significantly upregulated in the DL group compared to the control group ($P < 0.05$).

3.4 Serum levels of proinflammatory cytokines and oxidant stress

The effects on the inflammatory and oxidative parameters in the serum of rats treated with DahA are presented in Table 1. After intratracheal instillation for 4 weeks, the serum activity of SOD showed a significant decrease in the exposed groups, and the level of serum IL-6 was significantly upregulated in the DH group compared to the control group ($P < 0.05$). Meanwhile, the levels of serum MDA and TNF-α were also upregulated, although not significantly, in the exposure groups ($P > 0.05$).

3.5 Oxidants and anti-oxidants in rat lung tissue

As shown in Table 1, compared with the control group, the levels of iNOS and NO in the DH group and MDA in the DL group in the lungs of rats were significantly increased ($P < 0.05$), while SOD activity was markedly inhibited in the exposed groups ($P < 0.05$). Additionally, the level of eNOS in the exposed groups was not statistically significantly different compared with the control group ($P < 0.05$).

3.6 RRLC/Q-TOF-MS fingerprinting and multivariate analysis

The PLS-DA score plot showed that the variation in R^2Y was 99.1%, while the variation in Q^2 was 87.0% in ESI+ mode, indicating that the model had good fitting and prediction ability. A permutation test with 800 permutations was performed, which showed that the R^2 and Q^2 values were lower than the original points to the right, and the Q^2 regression line had a negative intercept, confirming that the PLS-DA model was valid (Fig. 2).

3.7 Alterations of pulmonary metabolome

This study indicated that DahA exposure disrupted the pulmonary metabolome in rats, and 13 differential metabolites were identified as biomarkers (Table 2). The upregulated clusters included Prolyl-Tryptophan and Docosahexaenoic acid (DHA). The downregulated cluster included LysoPC (22 ： 6), LysoPE (0 ： 0/20 ： 0), phosphatidylethanolamine (PE)-NMe (18:1), phosphatidic acid (PA) (i-13 ： 0/i-12 ： 0), 3-O-Sulfogalactosylceramide, sphingomyelin (SM) (d18 ： 0/20 ： 0), Carbamoyl phosphate (CP), Dihydrofolic acid, Choline, Glutamylglycine, and Isoleucyl-Glutamate (Fig. 3).

3.8 Pathway Analysis

The potential target metabolic pathway analysis using MetaboAnalyst 3.0 revealed that three metabolic pathways—folate biosynthesis, glycerophospholipid metabolism, and nitrogen metabolism—were the most significant pathways (Fig. 4).

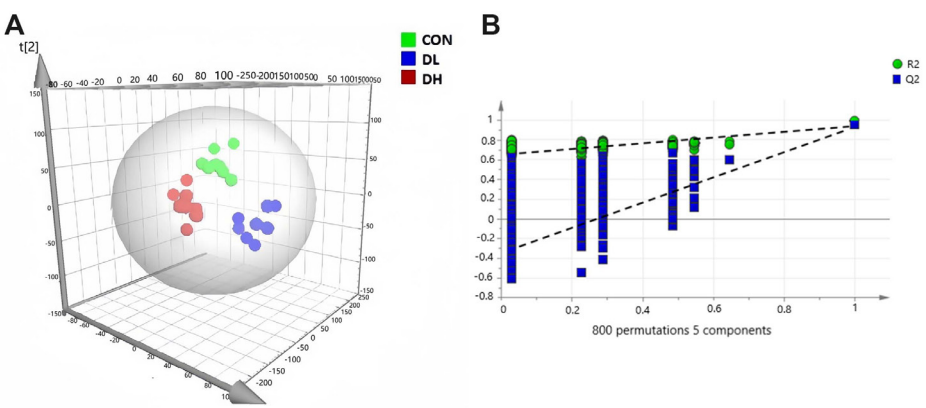

Fig. 2 Score plot with PLS-DA and permutation test of serum metabolites in control (CON) and exposure groups

Panel (A) shows the score plot derived from PLS-DA analysis, while panel (B) presents the results of the permutation test, comparing the serum metabolite profiles between the CON and exposure groups.

Table 2 Important metabolites in RRLC/Q-TOF-MS positive ion modes (ESI+)

NO.	VIP	RT	Actual mass	Exact mass	Mass error (ppm)	Molecule composition	Idetity	Adduct	Pathway
1	1.934	17.819	780.543	780.554	14.374	C44H78NO8P	PE-NMe (18:1/20:4)	M+H	Glycerophospholipid metabolism
2	1.854	17.999	104.106	104.108	11.371	C5H14NO	Choline	M+H	Gly, serine and threonine metabolism
3	1.835	18.452	205.086	205.082	-16.249	C7H12N2O5	Glutamylglycine	M+H	Gly, serine and threonine metabolism
4	1.832	27.710	141.990	141.991	1.562	CH4NO5P	Carbamoyl phosphate	M+H	Nitrogen metabolism
5	1.826	15.024	444.169	444.163	-13.058	C19H21N7O6	Dihydrofolic acid	M+H	Folate biosynthesis
6	1.800	20.461	551.376	551.371	-8.524	C28H55O8P	PA (i-13:0/i-12:0)	M+H	Glycerophospholipid metabolism
7	1.788	22.563	806.556	806.545	-13.252	C42H79NO11S	3-O-Sulfogalactosylceramide	M+H	Sphingolipid metabolism
8	1.787	18.439	302.144	302.151	21.161	C16H19N3O3	Prolyl-Tryptophan	M+H	Tryptophan metabolism
9	1.734	21.066	329.244	329.247	9.112	C22H32O2	Docosahexaenoic acid	M+H	Unsaturated fatty acid metabolism
10	1.675	24.426	761.642	761.654	15.602	C43H89N2O6P	SM (d18:0/20:0)	M+H	Sphingolipid metabolism
11	1.654	16.147	568.335	568.340	9.015	C30H50NO7P	LysoPC (22:6)	M+H	Lysophospholipid metabolism
12	1.638	18.365	510.353	510.356	5.878	C25H52NO7P	LysoPE (0:0/20:0)	M+H	Lysophospholipid metabolism
13	1.615	11.930	261.145	261.145	0	C11H20N2O5	Isoleucyl-Glutamate	M+H	Nitrogen metabolism

PE:phosphatidylethanolamine; PA: phosphatidic acid; SM: sphingomyelin.

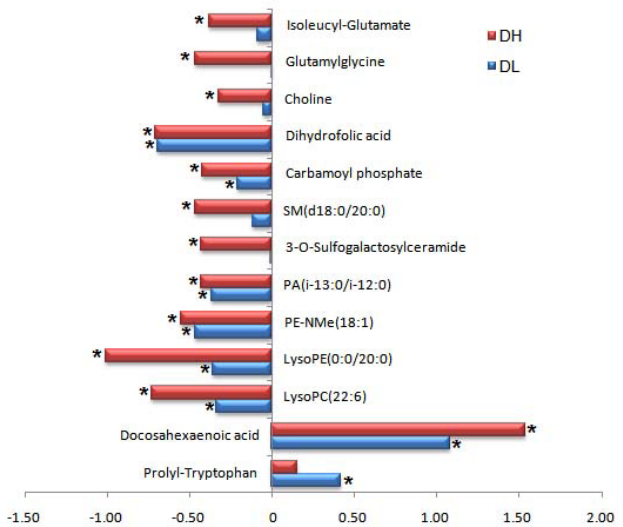

Fig. 3 Trends in alterations of different metabolites in serum comparing DahA exposed groups with the control group

The horizontal axis represents the ratio of the metabolite in the exposure group compared with the control group, calculated as ($C_{exposed}$ - $C_{control}$) / $C_{control}$. This plot illustrates the changes in metabolite levels following DahA exposure.

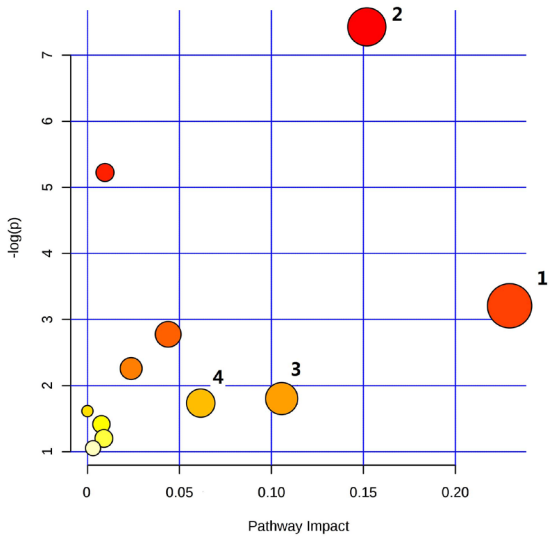

Fig. 4 Pathway analysis of biomarkers using MetaboAnalyst 3.0

(1) Folate biosynthesis; (2) Glycerophospholipid metabolism; (3) Nitrogen metabolism; (4) Sphingolipid metabolism. The analysis highlights key metabolic pathways impacted by DahA exposure, identifying potential biomarkers associated with pulmonary toxicity.

4 Discussion

The results showed that cytotoxicity markers (LDH, AKP, TP) in BALF significantly increased. Moreover, inflammatory cell infiltration and proliferation of fibrous tissue were observed in the lungs of the exposure groups. Thus, it can be concluded that the toxicity of DahA may cause acute lung injury in treated rats. It is well known that under stress conditions, the activities of antioxidative enzymes such as SOD may be inhibited, while excessive ROS can damage the cell membrane and form MDA[18]. Additionally, excessive NO, regulated by iNOS, may generate more toxic peroxynitrite anions[20], causing oxidative damage and cytotoxicity[21]. Therefore, we examined the concentrations of SOD, MDA, iNOS, eNOS, and NO in rat lung tissue and serum. The results of this study demonstrated that exposure to DahA may induce oxidative stress by inhibiting SOD activity and elevating iNOS activity as well as the levels of MDA and NO. The generation of ROS/RNS, in turn, may induce the release of proinflammatory cytokines and chemokines, leading to lung injury. Furthermore, we examined the concentrations of TNF-α and IL-6 in rat serum and BALF, and the results indicated that lung inflammatory injury was induced, accompanied by increased levels of pro-inflammatory cytokines such as IL-6. Therefore, the

metabolic changes associated with early damage caused by DahA toxicity must be elucidated in future studies on the toxicity mechanisms of PAHs in the environment.

In the present study, serum metabolomics of DahA exposure were analyzed using RRLC/Q-TOF-MS. Thirteen principal serum metabolites were identified as contributors to the clusters. The serum metabolomic changes indicated that exposure to DahA can affect inflammatory responses and oxidative stress factors in the lung by disrupting folate biosynthesis, lipid metabolism, nitrogen metabolism, and amino acid metabolism. The flow diagram illustrates the main pathways and toxic effects of metabolic changes caused by DahA exposure (Fig. 5).

This study demonstrated that DahA exposure could trigger an increase in oxidized phospholipids, mediating a systemic inflammatory response. Abnormal lipid metabolism is closely associated with the activation of oxidative and inflammatory pathways[22]. Metabolic disorders of glycerophospholipids and sphingomyelins were revealed in this study. Surfactant phospholipids, such as PA and PE, are essential components of cell membranes, which serve as critical structures for regulating the intercellular exchange of exogenous compounds[23]. Previous studies have shown that phospholipid metabolism plays a significant role in the pathogenesis of various diseases[18]. In inflamed lungs, lysophospholipids (lysoPC and lysoPE) are produced through the hydrolysis of phospholipids, leading to surfactant dysfunction[24]. LysoPC facilitates the entry of long-chain fatty acids, such as DHA, into mitochondria for fatty acid oxidation, producing acetyl-CoA, which participates in the tricarboxylic acid (TCA) cycle. This process can generate excessive ROS and impair antioxidant defenses[25].

Sphingolipids, essential components of membrane lipids, are involved in numerous cellular signaling pathways and play critical roles in cell death and survival[26]. SM, a primary sphingolipid component, plays a pivotal role in cellular responses to oxidative stress[13]. The observed reduction in serum SM and 3-O-sulfogalactosylceramide levels suggests that DahA exposure disrupts the membrane distribution of these components. SM is hydrolyzed into sphingosine, which is phosphorylated by sphingosine kinase and can mitigate tissue oxidative injury[27]. Results from KEGG pathway analyses further suggest that the decreased levels of 3-O-sulfogalactosylceramide and SM are indicative of lung-related disease progression, driven by inhibited sphingosine kinase activity and aggravated oxidative tissue damage. Taken together, the observed alterations in the serum glycerophospholipid and sphingolipid profiles in this study suggest that DahA exposure disrupts lipid metabolism, playing a crucial role in the pathogenesis of inflammatory diseases.

Plasma concentrations of glutamate, dihydrofolic acid, CP, and

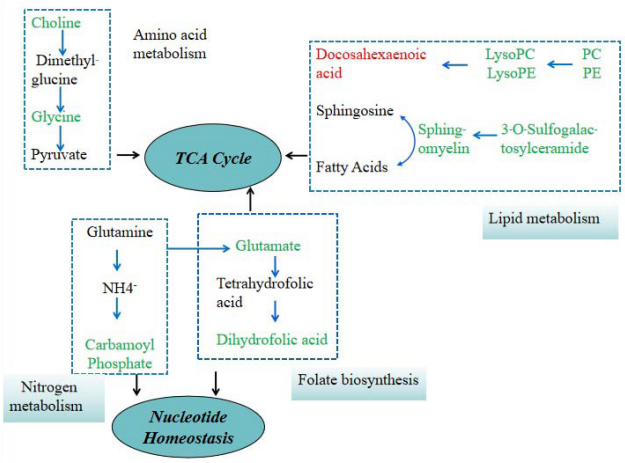

Fig. 5 Toxic effects of metabolic changes induced by DahA exposure
The serum metabolomic changes reveal that exposure to DahA disrupts key metabolic pathways, including folate biosynthesis, lipid metabolism, nitrogen metabolism, and amino acid metabolism. These disruptions contribute to heightened inflammatory responses and oxidative stress in the lungs, providing insight into the mechanisms underlying DahA-induced pulmonary toxicity.

dehydroascorbic acid were lower in the exposure groups compared to the control group, indicating that nitrogen metabolism and folate biosynthesis pathways were disrupted. By examining metabolic pathways in HMDB and KEGG, we identified glutamate as a crucial intermediate. Glutamate is produced from glutamine through the action of phosphate-dependent glutaminase. It is known to possess antioxidant activity, regulate body weight, and modulate hormone release[28]. Additionally, glutamate serves as a precursor for tetrahydrofolate synthesis. Tetrahydrofolate is converted into dihydrofolate by dihydrofolate reductase, a process critical for the transfer of one-carbon units involved in DNA methylation and nucleotide synthesis[29]. Thus, the observed decrease in dihydrofolic acid levels in this study may impair nucleotide homeostasis. Furthermore, glutamine is metabolized in mitochondria into ammonia and glutamate. Ammonia, along with bicarbonate, contributes to the synthesis of CP in mitochondria[30]. CP plays a vital role in pyrimidine and purine synthesis, and its reduction can interfere with nucleotide synthesis, compromise S-phase progression, and lead to DNA damage. Additionally, CP serves as a substrate for the synthesis of arginine and urea during de novo pyrimidine synthesis in the mammalian liver[31]. Thus, a reduction in CP concentration not only affects nucleotide homeostasis but also disrupts the urea cycle. This study suggests that the disruption of folate biosynthesis and nitrogen metabolism impairs the activity of metabolic kinases and affects nucleotide homeostasis, ultimately promoting disease development.

Amino acid metabolism provides the material basis for protein synthesis and energy metabolism. In the current study, we observed

significantly higher serum levels of prolyl-tryptophan, while glutamylglycine and isoleucyl-glutamate were significantly lower in the exposure groups compared to the control group. Using HMDB and KEGG pathway analyses, we identified glycine as a key metabolite promoting glutathione (GSH) synthesis and playing a critical role in antioxidant defense during liver damage[32]. The observed decrease in glycine levels in this study suggests a weakened antioxidant system. Additionally, glutamate is known to mitigate inflammation induced by oxidative stress and enhance the TCA cycle, particularly in lipid and glucose metabolism[33]. Tryptophan, on the other hand, is integral to T-cell-mediated inflammation, and previous studies have shown that changes in serum tryptophan concentrations can trigger systemic inflammatory responses[34]. In this study, DahA exposure disrupted amino acid metabolism, which contributed to inflammation and oxidative stress.

To the best of our knowledge, this is the first report evaluating metabolic changes and exploring the mechanisms of DahA-induced pulmonary injury in rats using metabolomics techniques following intratracheal instillation. However, our study has some limitations. While intratracheal instillation is a widely accepted method in toxicological studies, it represents a non-physiological route of exposure, leading to nonuniform distribution of the instilled material. Therefore, the potential biomarkers identified in this study require further validation in future research.

5 Conclusions

In summary, our results suggest that DahA exposure induces pulmonary injury in rats following intratracheal instillation, potentially disrupting key metabolic pathways such as folate biosynthesis, glycerophospholipid metabolism, and nitrogen metabolism. Furthermore, these metabolic disorders may interfere with the TCA cycle and compromise nucleotide homeostasis, leading to heightened inflammatory responses and oxidative stress. These findings highlight a possible mechanism by which atmospheric particulate matter-bound PAHs exacerbate respiratory diseases, particularly during the heating season in cold regions. Although this was a preliminary study, we believe it is the first to identify potential biomarkers associated with DahA exposure and its toxicity, providing a foundation for further research into the health impacts of PAHs in environmental pollution.

Acknowledgments

Not applicable.

Research ethics

Prior to the study initiation, the experimental protocol was reviewed and approved by the Committee on Animal Research and Ethics of Harbin Medical University (2015010).

Informed consent

Not applicable.

Author contributions

Kang Z, Wang C, Na X L conceived and designed the study. Kang Z, Hong Q Q, Bai Y N and Yu T Y performed the experiments and data collection. Kang Z, Yan F and Liu X B analysed the data. Kang Z wrote and compiled the manuscript. All authors read and approved the final version of the manuscript.

Use of Large Language Models, AI and Machine Learning Tools

None declared.

Conflict of interest

The authors declare no competing interest in this study.

Research funding

This work was supported partly by the Research Foundation of Health and family planning commission in Heilongjiang (2016-272) and the Natural Science Foundation of Heilongjiang Province (LH2021H010).

Data availability

Data supporting the findings of this study are available from the corresponding author upon reasonable request.

References

[1] Patel A B, Shaikh S, Jain K R, *et al*. Polycyclic aromatic hydrocarbons: sources, toxicity, and remediation approaches. Front Microbiol, 2020; 11, 562813.

[2] Hertz-Picciotto I, Baker R J, Yap P S, *et al*. Early childhood lower

respiratory illness and air pollution. Environ Health Perspect, 2007; 115(10): 1510-1518.
[3] Jeng H A, Pan C H, Diawara N, *et al.* Polycyclic aromatic hydrocarbon-induced oxidative stress and lipid peroxidation in relation to immunological alteration. Occup Environ Med, 2011; 68(9): 653-658.
[4] Perera F P, Li Z, Whyatt R, *et al.* Prenatal airborne polycyclic aromatic hydrocarbon exposure and child IQ at age 5 years. Pediatrics, 2009; 124(2): e195-e202.
[5] Perera F, Herbstman J. Prenatal environmental exposures, epigenetics, and disease. Reprod Toxicol, 2011; 31(3): 363-373.
[6] Wassenberg D M, Di Giulio R T. Synergistic embryotoxicity of polycyclic aromatic hydrocarbon aryl hydrocarbon receptor agonists with cytochrome P4501A inhibitors in Fundulus heteroclitus. Environ Health Perspect, 2004; 112(17): 1658-1664.
[7] Kim A, Park M, Yoon T K, *et al.* Maternal exposure to benzo[b] fluoranthene disturbs reproductive performance in male offspring mice. Toxicol Lett, 2011; 203(1): 54-61.
[8] Kummer V, Mašková J, Matiašovic J, *et al.* Morphological and functional disorders of the immature rat uterus after postnatal exposure to benz[a]anthracene and benzo[k]fluoranthene. Environ Toxicol Pharmacol, 2009; 27(2): 253-258.
[9] IARC Working Group on the Evaluation of Carcinogenic Risks to Humans. Some non-heterocyclic polycyclic aromatic hydrocarbons and some related exposures. IARC Monogr Eval Carcinog Risks Hum, 2010; 92: 1-853.
[10] Kang Z, Liu, X B, Yang, C, *et al.* Effect of ambient $PM_{2.5}$-bound BbFA and DahA on small airway dysfunction of primary schoolchildren in northeast China. Biomed Res Int, 2019; 2019: 2457964.
[11] Malik A I, Rowan-Carroll A, Williams A, *et al.* Hepatic genotoxicity and toxicogenomic responses in Muta™Mouse males treated with dibenz[a,h]anthracene. Mutagenesis, 2013; 28(5): 543-554.
[12] Okona-Mensah K B, Battershill J, Boobis A, *et al.* An approach to investigating the importance of high potency polycyclic aromatic hydrocarbons (PAHs) in the induction of lung cancer by air pollution. Food Chem Toxicol, 2005; 43(7): 1103-1116.
[13] Wang X F, Jiang S F, Liu Y, *et al.* Comprehensive pulmonary metabolome responses to intratracheal instillation of airborne fine particulate matter in rats. Sci Total Environ, 2017; 592: 41-50.
[14] Xu Y Y, Wang W J, Zhou J, *et al.* Metabolomics analysis of a mouse model for chronic exposure to ambient $PM_{2.5}$. Environ Pollut, 2019; 247: 953-963.
[15] Zhang Y N, Li Y B, Shi Z X, *et al.* Metabolic impact induced by total, water soluble and insoluble components of PM acute exposure in mice. Chemosphere, 2018; 207: 337-346.
[16] He M, Ichinose T, Yoshida S, *et al.* $PM_{2.5}$-induced lung inflammation in mice: Differences of inflammatory response in macrophages and type II alveolar cells. J Appl Toxicol, 2017; 37(10): 1203-1218.
[17] Li R J, Kou X J, Xie L Z, *et al.* Effects of ambient $PM_{2.5}$ on pathological injury, inflammation, oxidative stress, metabolic enzyme activity, and expression of c-fos and c-jun in lungs of rats. Environ Sci Pollut Res Int, 2015; 22(24): 20167-20176.
[18] Roberts L D, Souza A L, Gerszten R E, *et al.* Targeted metabolomics. Curr Protoc Mol Biol, 2012; Chapter 30, Unit 30.2-30.2.24.
[19] Sun M, Gao X Q, Zhang D W, *et al.* Identification of biomarkers for unstable angina by plasma metabolomic profiling. Mol Biosyst, 2013; 9(12): 3059-3067.
[20] Snyder S H, Bredt D S. Biological roles of nitric oxide. Sci Am, 1992; 266(5): 68-71, 74-77.
[21] Virág L, Szabó E, Gergely P, *et al.* Peroxynitrite-induced cytotoxicity: mechanism and opportunities for intervention. Toxicol Lett, 2003; 11: 113-124, 140-141.
[22] Zhao Y Y, Wang H L, Cheng X L, *et al.* Metabolomics analysis reveals the association between lipid abnormalities and oxidative stress, inflammation, fibrosis, and Nrf2 dysfunction in aristolochic acid-induced nephropathy. Sci Rep, 2015; 5: 12936.
[23] Walker A K, Jacobs R L, Watts J L, at al. A conserved SREBP-1/phosphatidylcholine feedback circuit regulates lipogenesis in metazoans. Cell, 2011; 147(4): 840-852.
[24] Hite R D, Seeds M C, Safta A M, *et al.* Lysophospholipid generation and phosphatidylglycerol depletion in phospholipase A(2)-mediated surfactant dysfunction. Am J Physiol Lung Cell Mol Physiol, 2005; 288(4): L618-L624.
[25] Hu W Y, Dong T Y, Wang L L, *et al.* Obesity aggravates toxic effect of BPA on spermatogenesis. Environ Int, 2017; 105: 56-65.
[26] Sun H, Zhao J, Zhong D, *et al.* Potential serum biomarkers and metabonomic profiling of serum in ischemic stroke patients using UPLC/Q-TOF MS/MS. PloS one, 2017; 12(12): e0189009.
[27] Ebenezer D L, Fu P, Natarajan V. Targeting sphingosine-1-phosphate signaling in lung diseases. Pharmacol Ther, 2016; 168: 143-157.
[28] Iwatsuki K, Torii K. Peripheral chemosensing system for tastants and nutrients. Curr Opin Endocrinol Diabetes Obes, 2012; 19(1): 19-25.
[29] Salbaum J M, Kappen C. Genetic and epigenomic footprints of folate. Prog Mol Biol Transl Sci, 2012; 108: 129-158.
[30] Kim J, Hu Z, Cai L, *et al.* CPS1 maintains pyrimidine pools and DNA synthesis in KRAS/LKB1-mutant lung cancer cells. Nature, 2017; 546(7656): 168-172.
[31] Pausch J, Rasenack J, Häussinger D, *et al.* Hepatic carbamoyl phosphate metabolism. Role of cytosolic and mitochondrial carbamoyl phosphate in de novo pyrimidine synthesis. Eur J Biochem, 1985; 150(1): 189-194.
[32] Yuan L, Kaplowitz N. Glutathione in liver diseases and hepatotoxicity. Mol Aspects Med, 2009; 30(1-2): 29-41.
[33] Ni H, Lu L, Deng J, *et al.* Effects of glutamate and aspartate on serum antioxidative enzyme, sex hormones, and genital inflammation in boars challenged with hydrogen peroxide. Mediators Inflamm, 2016; 2016: 4394695.
[34] Waclawiková B, El Aidy S. Role of microbiota and tryptophan metabolites in the remote effect of intestinal inflammation on brain and depression. Pharmaceuticals, 2018; 11(3): 63.